Available online at www.sciencedirect.com

ScienceDirect

Physics Procedia 67 (2015) 976 – 981

Physics Procedia

25th International Cryogenic Engineering Conference and the International Cryogenic Materials Conference in 2014, ICEC 25–ICMC 2014

Magneto-elastic effect for 316LN-IG stainless steel at low temperature

A.V. Krivykh*, A.V. Irodova, V.E. Keilin

Kurchatov Institute, Kurchatov sq.1, Moscow 123182, Russia

Abstract

Tensile tests of 316LN-IG austenitic stainless steel samples cut out from tubes along their axis are carried out in liquid and gaseous helium below 7 K. The tubes were intended for conductor conduits for the toroidal magnet system for ITER. Time dependences of temperature, strain and strain induced magnetization normal to the sample surface are examined with respect to stress. A complicated behavior of the local deformation near slip bands is detected that seems as unloading and shrinking regions adjacent to slip planes. The magneto-elastic effect indicating a negative longitudinal magneto-striction for the initial γ phase and the α phase induced by strain is found. The events without local heat release when jumping strain are explained as a result of the magneto-caloric effect in the regions unloaded in slipping.

Peer-review under responsibility of the organizing committee of ICEC 25-ICMC 2014

Keywords: 316LN-IG stainless steel; low-temperature tensile tests; local deformation near slip bands; magnetoelastic properties

1. Introduction

316LN-IG stainless steel is austenitic and used widely in devices operating at liquid helium temperature. In particular, it is used for the manufacture of conductor conduits for the ITER magnet system [1]. Non-magnetic under normal conditions, it becomes magnetic at low temperature when strained [2]. The steel "as received" becomes magnetic at low temperature after plastic strain as a result of the γ→α martensitic transformation resulting in a formation of the magnetic α phase [3]. If the steel has undergone a pre-aging procedure by means of a strain and subsequent long annealing, a magnetization therein arises without any mechanical loading at liquid nitrogen

* Corresponding author. Tel.: +7-499-196-9539; fax: +7-499-196-1704.
E-mail address: Krivykh_AV@rrcki.ru

Peer-review under responsibility of the organizing committee of ICEC 25-ICMC 2014
doi:10.1016/j.phpro.2015.06.165

temperature [4]. As is known, appearance of magnetization is a sign of embrittlement of austenitic stainless steels, which results in development of cracks and is highly undesirable in exploiting an apparatus working under extreme conditions, such as nuclear reactors [5]. This is a problem also for devices working at liquid helium temperature, the more since a strain at this temperature may be uneven and can result in dynamic forces [6].

In this work we investigated the interrelation of magnetic, elastic and thermal effects arising in 316LN-IG stainless steel strained at liquid helium temperature.

2. Samples and methods

The studies were performed on stainless steel 316LN-IG (0.013% C; 11.5% Ni; 16.5 Cr; 2.0% Mn). The closest Russian analog is 03Cr17Ni13NMo3.

Samples were fabricated from tubes "as received" (with a diameter of 48 mm and thickness of approximately 2 mm) as well as from tubes after an aging procedure, i.e. a complete simulation of the processes of the production cycle for the manufacture of niobium-tin conductors for TF-coils of the ITER magnet system [1]. The aging process consisted in compression and 2.5% elongation of the tube, whereby its outer diameter was reduced from 48 mm to 43 mm. Then the tube was annealed in inert gas at 650 ºC for 200 hours and allowed to cool with the furnace. Samples were prepared in accordance with the requirements of ASTM E8M: cut out from tubes along their axis by water-jet cutting, had a base length of 50 mm, with a total length of 140 mm, and a width of 12.5 mm. A typical sample, a tube segment, before tensile tests is shown in Fig. 1, on the left.

Tensile tests were carried out in accordance with the requirements of ASME E1450 in liquid and gaseous helium below 7 K using the universal machine "Instron-1195". To create the low temperature the load-carrying cryostat with an allowable force up to 40 kN was used [7]. The mechanical rigidity of the machine with cryostat was $7.5 \cdot 10^{-2}$ μm/N, and the normal strain rate was $3 \cdot 10^{-4}$ s^{-1}.

During the tests the applied stress and strain, temperature and strain-induced magnetization of a sample were measured versus time. The stress was measured by a sensor located on the machine frame. For strain measurement an extensometer with a base of 10 mm and an accuracy of 0.2% was mounted directly on the sample to locate simultaneously strain jumps. The temperature was measured on the sample surface by carbon or germanium thermometers with an accuracy of 0.4%. A quick-response germanium thermometer can register fast temperature changes inaccessible to the carbon one, but was limited in working range up to 30 K. The magnetization was measured by a Hall probe (2.5×2.5 mm^2) fixed on the sample surface, that registered the normal component of the induced magnetic field. The X-ray phase analysis of the samples was carried out before and after the tests on Bruker diffractometer (CuK_α radiation) using the FullProf suite [8].

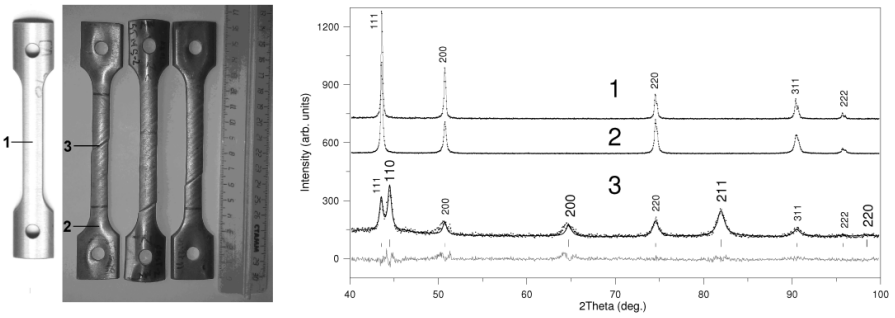

Fig. 1. (*On the left*) Photographs of segment samples for 316LN-IG stainless steel tubes "as received" (1) and after their tensile tests. Numbers mark regions where X-ray diffraction analysis was performed. (*On the right*) X-ray diffraction patterns (T=300 K, CuK_α) of the samples before (1) and after (2, 3) tensile tests at a temperature below 7 K. The regions 1, 2 and 3 where X-ray analysis was performed are shown *on the left*. In non-deformed (1) and low-deformed (2) regions only the γ phase with f.c.c. structure is present, a=3.602 Å. Numbers are indices of diffraction reflections, solid line connecting experimental points guides for the eye. In strongly deformed regions near slip bands (3) percentage of the γ phase, a=3.60 Å, is reduced to 20%, and 80% is the α phase with b.c.c. structure, a=2.88 Å. Points correspond to experimental curve, black solid line is calculated profile, below is the difference curve (grey line); positions and indices of diffraction reflections are marked by large symbols for the α phase and small ones for the γ phase.

3. Results and discussion

The appearance of the samples made from tubes "as received" after tensile tests until they rupture (see Fig. 1, on the left) indicates the jumping nature of plastic strain at helium temperature, as is evident from deep slip bands formed on the surface of the samples and a step of about 0.3 mm in the rupture point. (In the case of elastic strain, at nitrogen and higher temperatures, the samples remain uniform in length and a neck forms in the rupture point [9]). In most deformed regions intensive transformation of the γ phase in the magnetic α phase was detected (Fig. 1, on the right), in agreement with [6].

Typical time dependences of stress, strain and temperature as well as a fragment of the tensile stress-strain diagram for the samples tested in liquid helium are shown in Fig. 2. The upper limit of the elastic region corresponds to a relative strain of ε≈0.5%, and the elastic limit is σ≈1050 MPa. In the elastic region, the temperature on the sample surface does not change significantly. When strain changes from 0.5% to 1.2%, many small jumps appear on the stress curve σ(*t*) and the strain curve ε(*t*). At the same time, weak temperature pulses arise, which do not exceed 0.2 K and are increasing gradually with stress (Fig. 2, bottom).

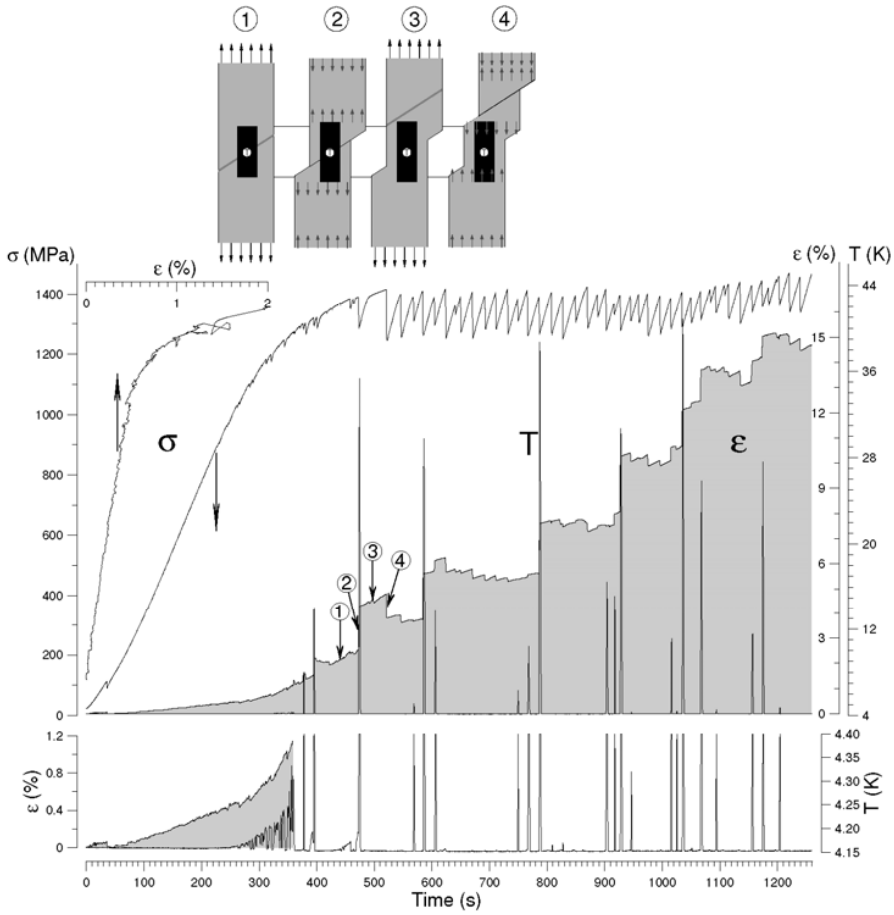

Fig. 2. Fragment of the tensile stress-strain diagram and time dependences of stress, strain and temperature for a tube segment tested in liquid helium. (σ) stress, arrows point to the horizontal axes corresponding to curves; (ε) unit strain for 10 mm region in the middle of the sample, below is the strain on a large scale for elastic and transitional to plastic ranges; (T) temperature taken by carbon thermometer on the sample surface in the strain region, below is temperature near 4 K on a large scale; horizontal axis is test time with step of 0.93 s. *Insert above*, schemes of deformation for the region under test corresponding to points 1, 2, 3 and 4 in the ε curve. The black rectangle is the region where strain is measured, and the white circle marked by T is the area where the temperature is measured. Arrows show stress (in schemes 1 and 3, grey lines correspond to subsequent slips) and an elastic force when stress drops as slip happens (in schemes 2 and 4).

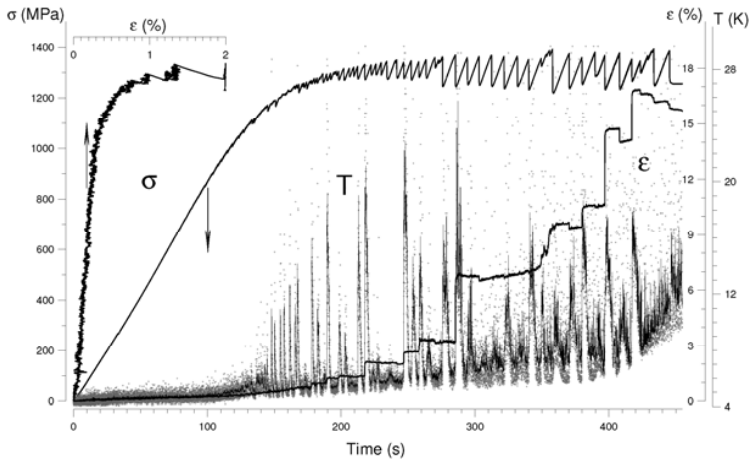

Fig. 3. Fragment of the tensile stress-strain diagram and time dependences of stress, strain and temperature for a tube segment tested in gaseous helium. (σ) stress, arrows point to the horizontal axes corresponding to curves; (ε) unit strain for 10 mm region in the middle of the sample; (T) temperature taken by a quick-response germanium thermometer on the sample surface in the strain region. Points correspond to measured quantities, solid line is a curve smoothed by three points. In the plastic range the data are doubtful because of large heat release; horizontal axis is test time with step of 0.02 s. Strain rate is $6 \cdot 10^{-4}$ s^{-1}.

The stress decreases rapidly with strain, and at ε=1.2% the value of $d\sigma/d\varepsilon$ becomes 20 times smaller than the Young's modulus (see the fragment of the tensile stress-strain diagram in Fig. 2). The material comes into a range of plastic strain. Since a transition to plastic strain means the beginning of transformation of the γ phase in the magnetic α phase [10], it is reasonable to relate the observed effects to the martensitic transformation. This deformation stage was traced in detail by testing in gaseous helium. In this case, the intensity of heat removal was two orders of magnitude less, which led to an increase by almost 150 times of the thermal effect (Fig. 3). To observe the temperature pulses separately we used a quick-response germanium thermometer which showed that the widths of the peaks do not exceed one second. In addition, following [11, 12] we increased the strain rate twice to intensify the martensitic transformation, which resulted in a more rapid transition to plastic strain (see the fragment of tensile stress-strain diagram Fig. 3) and an increase in frequency and amplitude of the jumps on the strain and stress curves in the transition region.

In the plastic range, when ε>1.2%, the strain shows jumps (which is evident from the stepped strain curve, Fig. 2). Each elongation of the sample by a jump is accompanied by a large heat release registered by the temperature sensor as temperature peak, the stronger the closer to the sensor a slip band runs. The width of such peaks is about 2.5 seconds, and their amplitude sometimes exceeds 40 K. In addition to the jumps leading to geometrical elongation of the sample by slips, small compression jumps are seen in the ε curve, which indicate an occurrence of regions where the sample undergoes local shrinking. Unlike the slip jumps, they are not accompanied by heat release, but coincide with stress drops as well (see Fig. 2), i.e. occur when the sample is unloading. The compression jumps are always preceded by a short time interval where the sample undergoes elastic stretching. Sometimes they follow directly the slip jumps. All this suggests that the compression jumps are caused by an elastic relaxation of regions adjacent to slips that have occurred outside the region where measurements are carried out (see the explaining insert in Fig. 2). In other words, the compressive jumps on the ε curve indicate that regions close to the slip band are unloading and shrinking when the slip occurs. The unloading time is about 10^{-4} s [7].

Simultaneous measurements of strain and magnetization carried out in liquid helium have shown (Fig. 4) that in the elastic region, where the sample contains only the γ phase, the normal component of the magnetic field arises on the sample surface. It increases when stretching the sample and decreases when unloading it. On the boundary of the elastic region, near ε≈0.6%, its value is 0.3 mT. Such behavior of magnetization indicates a negative longitudinal magnetostriction of the γ phase. In the transition from the elastic to plastic strain, where formation of the α phase starts, the strain-induced normal component of the magnetic field decreases, which can be reasonably explained with a screening of the magnetic field by the α phase.

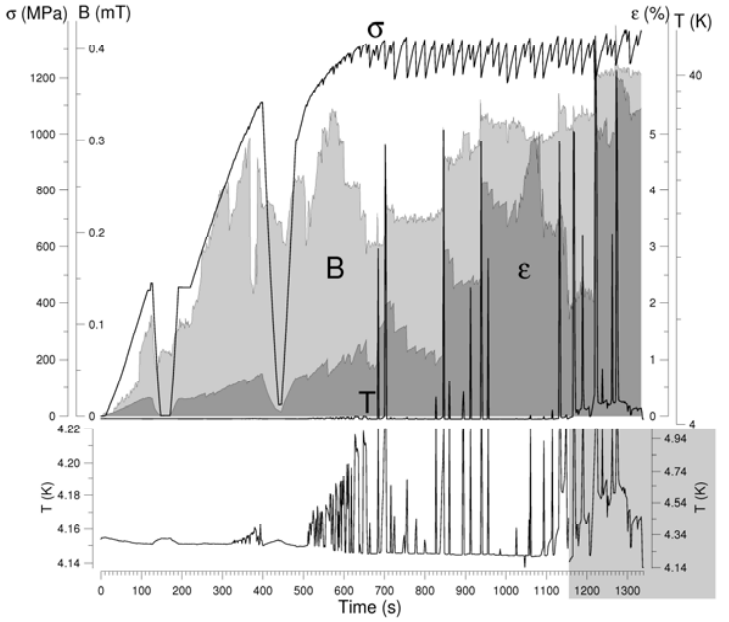

Fig. 4. Time dependences of stress, strain, temperature and strain induced magnetization for a tube segment tested in liquid helium. (σ) stress; (ε) unit strain for 10 mm region in the middle of the sample; (T) temperature on the sample surface in the strain region (logarithmic scale), below is the temperature near 4 K on a large scale for the test time up to 1150 s (left axis) and after 1150 s (right axis, grey field); (B) magnetic field normal to sample surface in the strain region; horizontal axis is test time with step of 1.74 s.

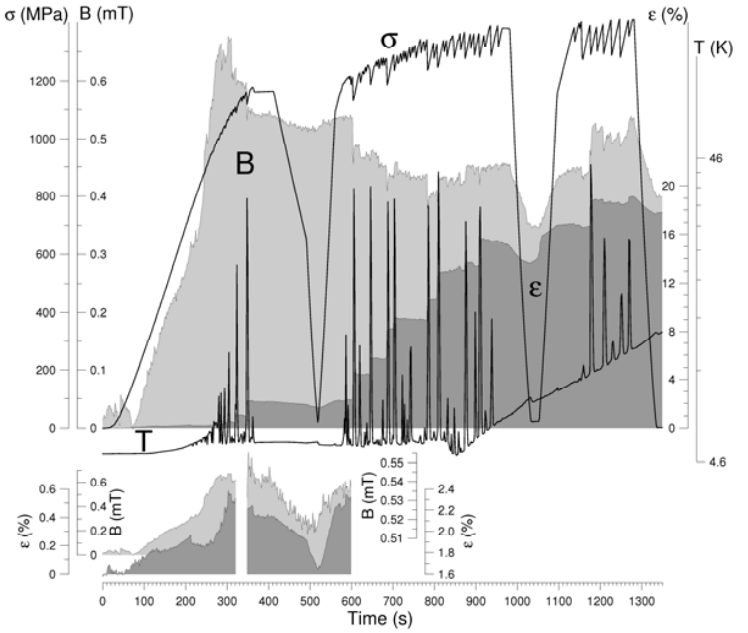

Fig. 5. Time dependences of stress, strain, temperature and strain induced magnetization for tube segment with weld tested in gaseous helium. (σ) stress; (ε) unit strain for 10 mm region near the weld; (T) temperature on the sample surface in the strain region (logarithmic scale); (B) magnetic field normal to sample surface in the strain region; below is the strain and the magnetic field on large scales for elastic range (left axes) and unloading region (right axes); horizontal axis is test time with step of 1.74 s.

In the plastic range, where the content of the α phase increases rapidly (see the caption to Fig. 1), the normal component of the magnetic field resumes its rising with strain. Unlike the elastic region, it is irregular mainly due to strain jumps (Fig. 4). In order to clarify the magneto-elastic properties of the α phase, we have examined the sample with a weld (Fig. 5). (Martensitic transformation in welds is more intense than in homogeneous material [13]). In addition to the γ phase, the weld contained about 10% of the α phase, according to X-ray phase analysis. The upper limit of the elastic region decreases to ε≈0.25%, and the limit of the transition range is ε≈0.55% (Fig. 5, bottom). In the elastic region the normal component of the magnetic field on the weld surface is proportional to strain and reaches 0.3 mT at the value of ε≈0.25%, 2.5 times smaller than for homogeneous samples. Unlike homogeneous samples, in the transition range it does not decrease with strain, continues rising and reaches 0.65 mT at ε≈0.55% (Fig. 5, bottom). This indicates that the α phase initially present in the weld has the same magneto-elastic properties as the γ phase. In this case a screening of the magnetic field by the secondary α phase which results from martensitic transformation is imperceptible as long as its content is small compared to the initial α phase, and will appear only when the martensitic transformation will be intense. Indeed, when jumping plastic deformation begins, a rapid decrease of the normal component of the magnetic field on the weld surface happens (see Fig. 5). However, as shown by unloading and subsequent loading of the sample, the magnetic field continues to follow the elastic part of strain, the upper limit of which increases to 0.5% (Fig. 5, bottom). The next unloading carried out after long plastic strain of the sample in order to maximize the content of the α phase in it has shown that the normal component of the magnetic field completely follows the strain, including its elastic part, the upper limit of which increases by almost seven times, up to 1.5–2% (see the time range t>900 s in Fig. 5). In other words, there is a magneto-elastic effect in the α phase, and its characteristics indicate a negative longitudinal magnetostriction, as in the γ phase.

4. Conclusion

1. In the range of the jumping plastic strain a complicated behavior of local deformation near slip bands is observed. Regions adjacent to slip bands are unloaded and shrink at the moment of the strain jump.

2. In the elastic and plastic ranges the magneto-elastic effect indicating a negative longitudinal magnetostriction for the initial γ phase and the strain-induced α phase is found.

3. Taking into account the magneto-elastic effect, a lack of local heating at strain jumps found in the previous work [14] can be explained by the magneto-caloric effect in regions unloaded at the jumps. Such situation is possible if energy needed for adiabatic reorientation of magnetic moments when stress drops is comparable with heat release in slip bands.

References

[1] Mitchell N, Bessette D, Gallix R, Jong C, Knaster J, Libeyre P, Sborchia C, Simon F. *IEEE Trans Appl Supercond* 2008; 18: 435-440.
[2] Obst B. Basic aspects of tensile properties. In: Seeber B, editor. *Handbook of Applied Superconductivity*, Bristol: Institute of Physics Pub.; 1998, pp. 969-993.
[3] Obst B, Nyilas A. *Mater Sci Eng* 1991; 137A: 141-150.
[4] Krivykh AV, Anashkin OP, Keilin VE, Diev DN, Dinisilov AS, Shcherbakov VI, Tronza VI. *Preprint IAE-6674/10*, Moscow: Kurchatov Institute, 2011 (in Russian).
[5] Azhazha VM, Desnenko VA, Ozhigov LS, Azhazha ZhS, Svechkaryov IV, Fedorchenko AV. *Problems of Atomic Science and Technology, series: Physics of Radiation Effects and Radiation Materials Science* 2009; 94: 241-246 (in Russian).
[6] Anashkin OP, Keilin VE, Krivykh AV, Diev DN, Dinisilov AS, Shcherbakov VI, Tronza VI. *Adv Cryog Eng* 2012; 58: 117-124.
[7] Krivykh AV, Anashkin OP, Keilin VE, Diev DN, Dinisilov AS, Shcherbakov VI, Tronza VI. *Tech Phys* 2012; 57: 1562-1568.
[8] Roisnel T, Rodriguez-Carvajal J. A Windows tool for Powder Diffraction Pattern Analysis. *Mater Sci Forum* 2001; 378–381: 118-123.
[9] Wigley DA. *Mechanical Properties of Materials at Low Temperatures*, New York: Plenum Press; 1971.
[10] Skoczen B. Constitutive model of plastic strain induced phenomena at cryogenic temperatures. *J Theor Appl Mech* 2008; 46: 949-971.
[11] Hecker SS, Stout MG, Staudhammer KP, Smith LJ. Effects of Strain State and Strain Rate on Deformation-Induced Transformation in 304 Stainless Steel: Part I. Magnetic Measurements and Mechanical Behavior. *Met Mater Trans* 1982; 13A: 619-626.
[12] Murr LE, Staudhammer KP, Hecker SS. *Met Mater Trans* 1982; 13A: 627-635.
[13] Porter DA, Easterling KE. *Phase Transformations in Metals and Alloys*, London: Chapman & Hall; 1992.
[14] Krivykh AV, Anashkin OP, Keilin VE, Diev DN, Poliakov AV, Shcherbakov VI. *Proc. Int. Sci.-Tech. Conf. Nanotechnologies of Functional Materials (NFM'12)*, St. Petersburg, Russia, 2012, pp. 235-240 (in Russian).